# Molecular dynamics simulations of solid-phase epitaxy of Si: Defect formation processes

Shinji Munetoh, Koji Moriguchi, and Akira Shintani*

*Electronics Engineering Laboratories, Sumitomo Metal Industries, Ltd., 1-8 Fusocho, Amagasaki, Hyogo 660-0891, Japan*

Ken Nishihira and Teruaki Motooka

*Department of Materials Science and Engineering, Kyushu University, Hakozaki, Fukuoka 812-8581, Japan*

We have investigated defect formation processes during solid-phase epitaxy of Si in the [001] direction based on molecular dynamics (MD) simulations using the Tersoff potential. Two different types of defect formation processes have been successfully observed in the MD simulations. They can be characterized by the structure of Si-Si dimer bonds created at the amorphous/crystalline interface in the initial stage of the defect formation. In the first type, the Si-Si dimer bonds form coupled dimer lines and these coupled dimer lines lead to the creation of {111} stacking faults. In the second type, the Si-Si dimer bonds form a single dimer line which leads to the creation of [111] twins.

## I. INTRODUCTION

Silicon is one of the most important semiconductors for the substrate of microelectronic devices. In order to improve electric characteristics of Si substrate, the ion implantation has been adopted in the semiconductor manufacturing processes. Though ion implantation has an advantage for controlling of dopant profiles, it induces defect formation and amorphization in the implanted region. These defects are thermally removed and transformed to a crystalline state in the practical device fabrication.[1] In the recrystallized region, however, some defects such as dislocations and twins are found to remain.[2] It is extremely difficult to directly observe these phenomena and thus the microscopic mechanism of the crystallization and/or defect formation processes have not been well understood.

The molecular dynamics (MD) simulation is a powerful tool for studying the process of crystal growth. Recently, we reported crystal growth processes during solid-phase epitaxy (SPE) of Si in the [001] direction based on MD simulations using the Tersoff potential,[3] and successfully observed atomistic crystallization processes. In addition, we have found that the calculated activation energy of SPE at lower temperatures is in good agreement with the experimental value ($\approx 2.7$ eV), while it becomes lower at higher temperature. However, we could not observe the defect formation in the previous work. To the authors' best knowledge, there is no report on the atomistic defect formation process, though many researchers have performed MD simulations of Si crystallization.[4,5] In this paper, we have carried out large-scale MD simulations of solid phase epitaxy of Si, and further investigated defect formation processes during SPE in the [001] direction.

## II. CALCULATION METHOD

MD simulation have been performed using a large MD cell including approximately 10 000 Si atoms. Atomic movements were determined by solving the following Langevin equations:

$$m\ddot{\mathbf{r}}_i(t) = \mathbf{F}_i(t) - m\gamma\dot{\mathbf{r}}_i(t) + \mathbf{R}_i(t), \qquad (2.1)$$

where $m$ is the atomic mass, $\mathbf{r}_i(t)$ the position vector of the $i$th atom at time $t$, $\mathbf{F}_i(t)$ the interatomic force calculated by the Tersoff potential,[6,7] $\gamma$ the friction constant, and $\mathbf{R}_i(t)$ is a random force to control the temperature of systems considered, respectively. We employed the scheme developed by van Gunsteren and Berendsen[8] for numerical integrations of the Langevin equation. The time step for the integration and friction constant $\gamma$ were set at 2 fs and 5 ps$^{-1}$, respectively. While the Tersoff potential is well known that it gives rise to high melting temperature 2547 K,[9] it can well reproduce the structural properties of amorphous Si($a$-Si) (Ref. 10) and liquid Si ($l$-Si).[11,12]

At first, we examined melting temperature of bulk $a-$Si obtained by rapid quenching of liquid Si with the cooling rate of $10^{12}$ K/sec.[10] Figure 1 shows mean-square displacement (MSD) for various temperatures. No appreciable MSD can be observed at temperatures less than 2100 K suggesting that melting temperature is lager than 2100 K instead of
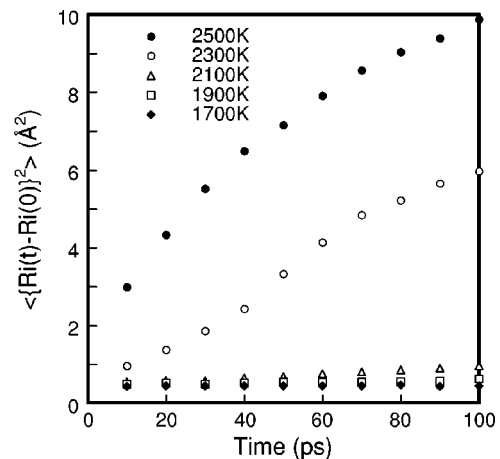


FIG. 1. Average mean-square displacements (MSD) of bulk $a$-Si for various temperatures. The bulk $a$-Si has been prepared by the cooling rate of $10^{12}$ K/s.
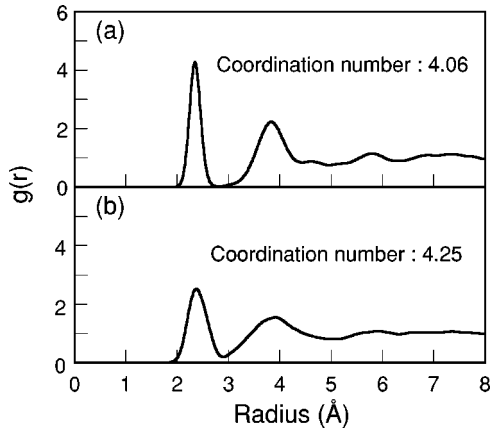
FIG. 2. Radial distribution functions (RDF's) of a bulk $a$-Si (a) at 0 K, (b) at 2000 K.

1700 K as was previously suggested.[10] The difference of melting temperature estimated can be attributed to superheating and supercooling which can be frequently observed in MD simulations due to finite simulation size effects. In general, accurate predictions of melting temperatures are by no means trivial to obtain in the direct simulations of phase transitions using the method of simply heating the system at constant volume or even constant pressure. This is because finite size effects and free energy barriers separating the phases involved lead to hysteresis in the direct simulations.

Figure 2 shows the radial distribution functions (RDF's) of $a$-Si at 0 and 2000 K along with the mean coordination number. The mean coordination number has been calculated by integrating associated RDF. The coordination numbers of the present bulk model of $a$-Si are estimated by 4.09 and 4.25 at 0 and 2000 K, respectively, which are close to that of crystalline Si ($c$-Si,4.0) and much lower than that of $l$-Si (4.6~5.0) by Cook and Clancy.[9] Therefore, we believe that the present MD simulations can demonstrate atomistic processes in Si SPE growth even at 2000 K. Detailed comments on the atomic diffusion properties near the $a/c$ Si(100) interface during SPE based on the same MD techniques have been presented elsewhere.[13]

The initial amorphous/crystal ($a/c$) interface was prepared using the same technique in the previous work,[3] that is by attaching eight $c$-Si(001) layers to a block of bulk $a$-Si. The original MD cell of $a$-Si was set to $21.7 \times 21.7 \times 43.4$ Å$^3$ and the number of Si atoms was 1024, which were determined by using the $c$-Si density, 2.33 g/cm$^3$. In order to investigate defect formation processes during SPE, we have used a larger MD cell with a size of $65.1 \times 65.1 \times 43.4$ Å$^3$ made by combining nine $a$-Si MD cells described above. The total number of atoms in the MD cell was 9920. The MD cell was pre-annealed at 1000 K for 20 ps and then heated at 2000 K. Periodic boundary conditions were employed in the [100] and [010] directions. In the [001] or $z$ direction, the top two layers of the single crystal region were fixed, while the bottom of the MD cell was assumed to be a free surface.

## III. RESULTS AND DISCUSSION

In this simulation, we have succeeded in observing two different types of defect formation processes. Figure 3 shows
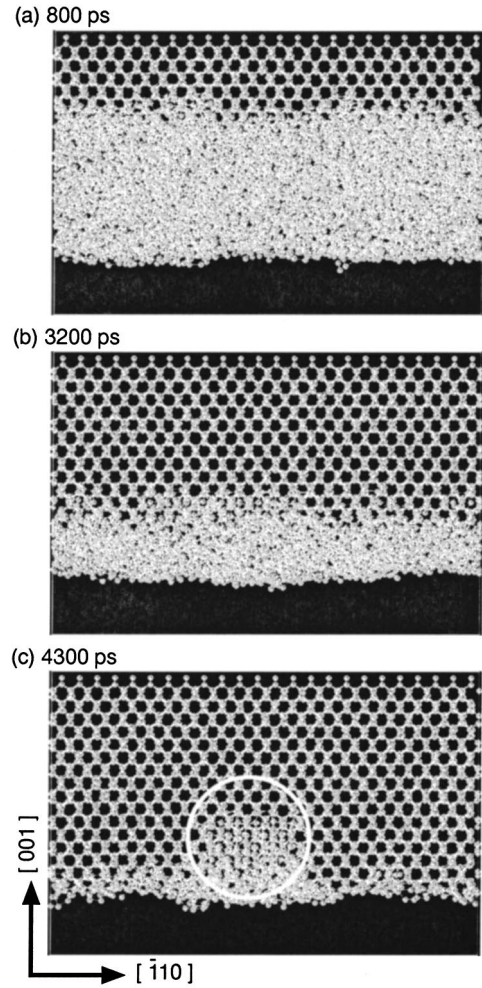


FIG. 3. The snapshots of the atomic arrangements during SPE of Si obtained by MD simulations at 2000 K: (a) after 800 ps, (b) after 3200 ps, and (c) after 4300 ps. Atomic positions in these figure were projected on the (110) plane. A misoriented part was observed at 4300 ps in the regions encircled.

an example of these processes during crystal growth observed by projecting atomic positions on the (110) plane. As the annealing time increases, the locations of the $a/c$ interface move down and the crystallization occurs. The crystallized region enclosed in Fig. 3(c) includes a misoriented part. To obtain more detailed structures of the defect, Figure 4 shows magnified pictures of the misoriented part, which are given by projecting the atomic positions on the [110], [$\bar{1}$10], and [001] planes. During annealing at 2000 K, five-membered rings are created at the $a/c$ interface which results in Si-Si dimer bonds formation [arrows in Fig. 4(b)]. It should be noted that these dimer bonds form a coupled dimer lines in the [$\bar{1}$10] direction as can be seen in the [001] view in Fig. 4(b). This structures resembles the $2 \times 1$ reconstructed Si(001) surface. These coupled dimer lines lead to the creation of {111} stacking faults as shown in the region enclosed by the solid lines in the [$\bar{1}$10] view in Fig. 4(c).

Figure 5 shows another example of defect formation processes found in the present simulations. In this case, the de-
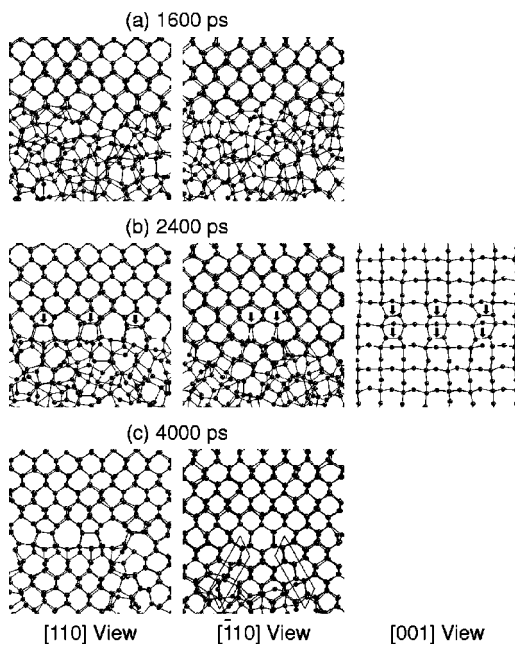
FIG. 4. Magnified pictures of the misoriented part encircled in Fig. 2(c). Si-Si bonds have been observed to form a coupled dimer lines in the $[\bar{1}10]$ direction at 2400 ps [arrows in (b)]. They lead to the creation of {111} stacking faults in the region enclosed by the solid lines in the $[\bar{1}10]$ view.

fect formation can be seen after 3200 ps. The Si-Si dimer bonds are also formed at the $a/c$ interface [arrows in Fig. 5(b)], but these dimer bonds form a single dimer line as shown in the [001] view in Fig. 5(b). This dimer line leads to the creation of hexagonal layers [solid line in the $[\bar{1}10]$ view in Fig. 5(c)] and twins [arrows in $[\bar{1}10]$ view in Fig. 5(c)]. In addition, some ring defects such as five- and seven-membered rings are formed [stars in the $[\bar{1}10]$ view in Fig. 5(c)]. This defect structure also resembles that of the 30° partial dislocation.

Khor and Sarma[14] performed MD simulations of the reconstruction of (001) Si surface using Tersoff potential, and shown that energies and bond lengths of the $2 \times 1 \mathrm{Si}(001)$ dimer bonds were in good agreement with total-energy density-functional calculations and dimer bonds were stable. Therefore, the $\langle 110 \rangle$ dimer bonds at the $a/c$ interface are also assumed to be stable and tend to lead to the creation of the misorientated part during crystal growth.

## IV. CONCLUSIONS

We have investigated defect formation processes during SPE of Si in the [001] direction based on MD simulations
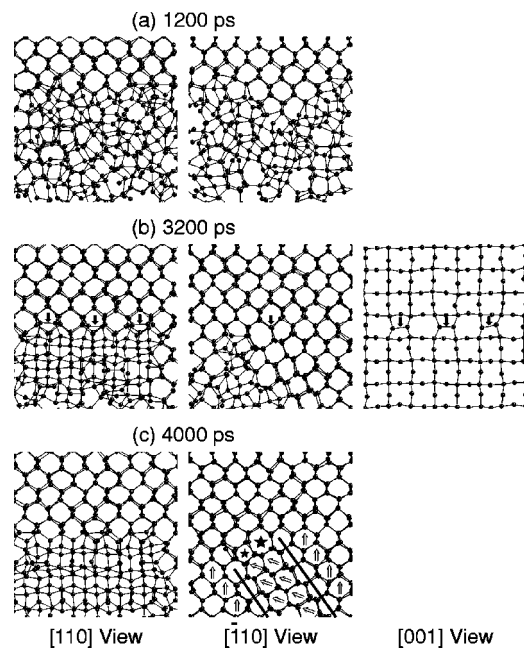


FIG. 5. Another example of defect formation processes. Si-Si bonds have been observed to form a dimer line in the $[\bar{1}10]$ direction at 3200 ps [arrows in (b)]. This dimer line leads to the creation of [111] twins [arrows in (c)] and five- and seven-membered rings [stars in (c)]. This structure resembles that of the 30° partial dislocation.

using the Tersoff potential. Two different types of defect formation processes have been successfully observed in the MD simulations. They can be characterized by the structure of Si-Si dimer bonds created at the $a/c$ interface in the initial stage of the defect formation. In the first type, the Si-Si dimer bonds form a coupled dimer lines and these coupled dimer lines lead to the creation of {111} stacking faults. In the second type, the Si-Si dimer bonds form a single dimer line which leads to the creation of [111] twins.

*Present address: Optoelectronics Technical Div. 1, Toyota-Gosei Co., Ltd., 710 Origuchi, Shimomiyake, Heiwa-cho, Nakashima-gun, Aichi 490-1312, Japan.

[1] W.C. Sinke, A. Polman, S. Roorda, and P.A. Stolk, Appl. Surf. Sci. **43**, 128 (1989).

[2] T. Cai, J. Appl. Phys. **67**, 7176 (1990).

[3] T. Motooka, K. Nishihira, S. Munetoh, K. Moriguchi, and A.

Shintani, Phys. Rev. B **61**, 8537 (2000).

[4] M.J. Uttormark, M.O. Thompson, and P. Clancy, Phys. Rev. B **47**, 15 717 (1993).

[5] U. Landman, W.D. Luedtke, R.N. Barnett, C.L. Cleveland, M.W. Ribarsky, E. Arnold, S. Ramesh, H. Baumgart, A. Martinez, and B. Khan, Phys. Rev. Lett. **56**, 155 (1986).

[6] J. Tersoff, Phys. Rev. B **38**, 9902 (1988).

[7] J. Tersoff, Phys. Rev. B **39**, 5566 (1989).

[8] W.F. van Gunsteren and H.J.C. Berendsen, Mol. Phys. **45**, 637 (1982).

[9] S.J. Cook and P. Clancy, Phys. Rev. B **47**, 7686 (1993).

[10] M. Ishimaru, S. Munetoh, and T. Motooka, Phys. Rev. B **56**, 15 133 (1997).

[11] M. Ishimaru, K. Yoshida, and T. Motooka, Phys. Rev. B **53**, 7176 (1996).

[12] M. Ishimaru, K. Yoshida, T. Kumamoto, and T. Motooka, Phys. Rev. B **54**, 4638 (1996).

[13] T. Motooka, K. Nishihira, S. Munetoh, K. Moriguchi, and A. Shintani, Phys. Rev. B **64**, 237402 (2001).

[14] K.E. Khor and S.D. Sarma, Phys. Rev. B **36**, 7733 (1987).